SEARCH FOR LUNAR VOLATILES USING THE LUNAR ORBITER LASER ALTIMETER AND THE DIVINER LUNAR RADIOMETER. E. A. Fisher [1], P. G. Lucey [1], M. Lemelin [1], B. Greenhagen [2], M. Siegler [3], E. Mazarico [4], G. A. Neumann [4], D. E. Smith [5], M. T. Zuber [5], [1]Hawaii Institute of Geophysics and Planetology, University of Hawaii at Manoa, 1680 East-West Rd, Honolulu, HI 96822, Fisher.ElizabethAnne@gmail.com, [2]JHU APL, Laurel, MD 20723, [3]Planetary Science Institute, Tuscon, AZ 85719, [4]NASA/Goddard Space Flight Center, Greenbelt, MD 20771, [5]Earth, Atmospheric and Planetary Sciences, MIT, Cambridge, MA 02139.

Introduction: The identification of surface ice at Mercury's poles relied largely on correlating anomalously bright surface material identified with surface reflectance measurements from the Mercury Laser Altimeter [1] with model temperatures that allow surface ice to be stable for billions of years [2]. A similar data set exists for the lunar poles. The Lunar Orbiter Laser Altimeter (LOLA) aboard the Lunar Reconnaissance Orbiter (LRO) provides surface reflectance measurements in the polar regions [3,4] and the Diviner Lunar Radiometer Experiment provides direct measurement of surface temperature. This enables a search for temperature dependent phenomena in the lunar polar regions. Diviner provides access to two types of temperature for each reflectance measurement: the maximum annual temperature and the instantaneous temperature at the time of a LOLA reflectance measurement. The maximum temperature a pixel experiences may govern irreversible or long-lived properties, e.g the degree of space weathering, or the presence of persistent frost deposits. Instantaneous temperature potentially provides access to reversible effects on surface reflectance, e.g. transient frost species or temperature-dependent optical properties of minerals. In this work we use newly calibrated LOLA reflectance data [5,6] to address temperature effects on reflectance in the polar regions.

Methods:

Datasets. Data used in this study include recently recalibrated normal albedo at 1.064 µm derived from LOLA reflectance measurements [5,6], simultaneously obtained measurements of instantaneous temperature derived from Diviner for this study, the maximum temperature experienced by each of the LOLA reflectance measurements' locations over the course of the LRO mission [7], and the local slope at those locations [5].

Analysis. Ideally, reversible temperature dependent effects would be sought by comparing the normal albedo of individual locations at different temperatures. However, the LOLA reflectance data set is limited over cold surfaces due to instrument challenges [4]. Therefore, comparisons among terrains involving instantaneous temperature were conducted statistically. Data utilized for this study were limited to latitudes at or within 20 degrees of each pole, and excluded the immediate pole within 2 degrees. Figures 1a, 1b and 2 are the average of albedo values in 2-degree temperature bins, plotted as a function of maximum or instantaneous temperature.

The Moon's reflectance is strongly correlated with slope [4], due to mass wasting removing darkened space weathered material from steep slopes. To mitigate this effect, we separated the data into a low-slope set (<10 degrees: little mass wasting, but strong space weathering), and a high-slope set (>20 degrees: strong mass wasting and weak space weathering) (Fig. 2).

Results: Figure 1a shows normal albedo as a function of maximum temperature for each pole. There

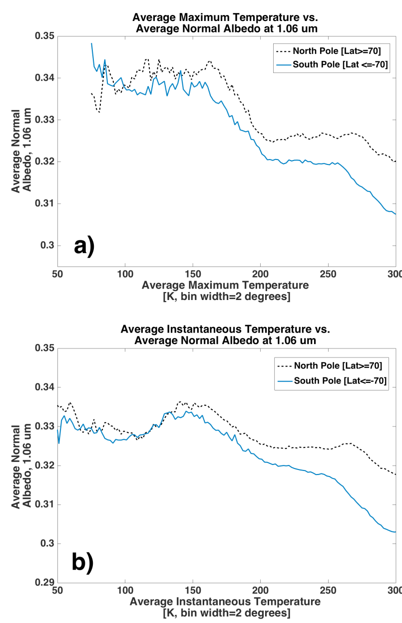

Figure 1. a) Comparison the behavior of average normal albedo as a function of average maximum temperature, and **b)** average normal albedo a function of instantaneous temperature, in the North and South.

is a general correlation between temperature and albedo. Furthermore, two portions of the curves show rapid increases in albedo with decreasing temperature, followed by a plateau. The onset of these increases occurs near ~270K and ~200K, with plateaus occurring between ~200 and ~250K and below ~150K. Finally, there is a notable lack of any changes in the curve near ~100K that might indicate the effect of persistent water ice.

Figure 1b is the instantaneous temperature equivalent of Figure 1a. We also observe an increase in albedo with decreasing instantaneous temperature, howev-

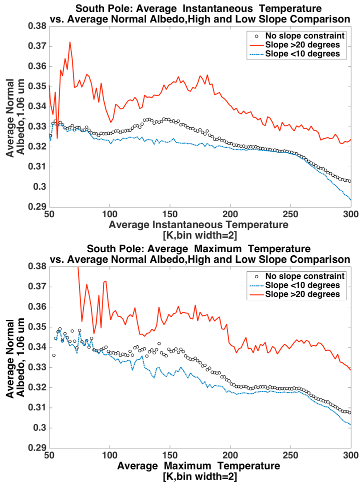

Figure 2. Plots comparing the behavior of high-slope (>20°) and low-slope (<10°) areas for normal albedo as a function of instantaneous temperature (top) and as a function of maximum temperature (bottom), for the South Pole.

er the details of the structure differ. The North Pole shows a much gentler slope than the South, and while the plateaus near 200-250K persist, the feature near ~150K resolves into a distinct peak at both poles.

Figure 2 shows the difference in behavior between low-slope and high-slope data for the South Pole. When albedo is plotted against instantaneous temperature, low-slope data (little mass wasting) shows a relatively steady increase in reflectance with decreasing temperature, with a strong break in slope near ~250K (Fig. 2). In contrast, high-slope data (less space weathering) shows no evidence of this change in behavior near ~250K, but prominently displays a peak in albedo near ~150K. When albedo is plotted against maximum temperature, these differences are muted, especially above 200K. Below 200K, the low-slope data shows a steady increase in albedo with decreasing temperature, whereas the high slope data shows a weak indication of a peak at 150K.

Discussion:

Space weathering effects. The general increase in normal albedo with decreasing maximum temperature observed at the poles can reasonably be attributed to space weathering. Previous studies have found that average surface albedo increases with latitude, likely because there is less solar wind sputtering at higher latitudes, leading to less space weathering [6,8]. Our data may reflect a polar extension of this trend.

Potential volatile deposition. We find a notable lack of clear excursions in normal albedo near ~100K that might be attributable to water ice. Therefore our analysis at this time does not support the presence of optically thick persistent frost deposits in the areas measured by LOLA.

However, the pattern of abrupt brightening with decreasing temperature followed by a plateau in albedo observed in the maximum temperature plots (Fig.1a) is consistent with deposition of a bright, stable volatile that persists for geologic time at lower temperatures. There are numerous simple organics with sublimation temperatures consistent with the observed rapid rises in albedo; coronene is a candidate for the albedo increase below ~300K and the plateau between ~200 and ~250K, and naphthalene for the albedo rise at ~200K and subsequent plateau at ~150K [9,10].

Instantaneous vs. maximum temperature. Because of some correlation between maximum and instantaneous temperature, caution must be applied in interpretation of albedo in terms of these two parameters. However, the difference in behavior of the albedo of shallow and steep slopes when plotted against each temperature parameter is suggestive of a real feature. While we have no explanation for the break in slope observed in the low-slope data (Fig. 2), the smooth nature of the curve could be a combination of previously mentioned space weathering effects, and potentially an intrinsic variation in the optical properties of materials [11], space weathering attenuating the latter effect.

Conclusions: We observe a general increase in normal albedo with decreasing temperature. This correlation between the normal albedo and the maximum temperature is consistent with a decrease in solar wind related space weathering products at high latitudes. Superimposed on this trend, the relationship between temperature and albedo at the lunar poles is strongly structured and may provide insight into the nature of lunar volatiles; we find strong increases in normal albedo at specific temperatures that may be caused by the deposition of stable volatiles. We observe no increase in normal albedo near ~100K, the approximate temperature at which water ice becomes stable on the lunar surface [9,10].

References: [1] Neumann G.A. et al. (2013) *Science, 339,* 296–300. [2] Paige D.A. et al. (2013) *Science, 339, 300*–303. [3] Smith D. E. et al. (2010) *Space Science Rev.,* 150, 209-241. [4] Lucey, P. G. et al. (2014) *Journal of Geophysical Research: Planets,* 119.7, 1665-1679. [5] Smith, D. E. (2015), LRO-L-LOLA-3-RADR-V1.0, NASA Planetary Data System.[http://pds-geosciences.wustl.edu/lro/lro-l-lola-3-rdr-v1/lrolol_1xxx/data/lola_radr/]. [6] Lemelin, M. et al. (2016) *Icarus-14476Rl*, accepted. [7] Williams, J.-P. et al., (2016) Icarus, submitted. [8] Hemingway, D.J. et al. (2015) *Icarus*, *261*, 66-79. [9] Siegler et al. (2014), abstracts to *LEAG.* [10] Zhang, J. A., & Paige, D.A. (2009) *Geophysical Research Letters*, *36*(16). [11] Hinrichs, J. L. & Lucey, P. G. (2002) *Icarus,* 155.1, 169-180.